Electric field simulation and measurement of a pulse line ion accelerator*

SHEN Xiao-Kang(申晓康)[1,2;1)] ZHANG Zi-Min(张子民)[1;2)] CAO Shu-Chun(曹树春)[1]
ZHAO Hong-Wei(赵红卫)[1] WANG Bo(王博)[3] SHEN Xiao-Li(沈晓丽)[3]
ZHAO Quan-Tang(赵全堂)[1;2)] LIU Ming(刘铭)[1] JING Yi(景漪)[1]

[1] Institute of Modern Physics, Chinese Academy of Sciences, Lanzhou 730000, China
[2] Graduate University of Chinese Academy of Sciences, Beijing 100049, China
[3] Department of Electrical Engineering, Tsinghua University, Beijing 100084, China

Abstract: An oil dielectric helical pulse line to demonstrate the principles of a Pulse Line Ion Accelerator (PLIA) has been designed and fabricated. The simulation of the axial electric field of an accelerator with CST code has been completed and the simulation results show complete agreement with the theoretical calculations. To fully understand the real value of the electric field excited from the helical line in PLIA, an optical electric integrated electric field measurement system was adopted. The measurement result shows that the real magnitude of axial electric field is smaller than that calculated, probably due to the actual pitch of the resister column which is much less than that of helix.

Key words: PLIA, accelerator, electric field measurement, sensor

PACS: 29.20.-c, 29.20.Ej **DOI:** 10.1088/1674-1137/36/7/016

1 Introduction

The motivation for the Pulse Line Ion Accelerator (PLIA) concept came from the high linear charge density ion beam requirements of high energy density physics and warm dense matter. A PLIA with constant parameter helical lines should result in an output energy much larger than the several hundred kilovolt peak voltages on the helix, with a goal of 3–5 MeV/m acceleration gradients. It has the potential to reduce the length of an equivalent induction accelerator by a factor of 6–10 while simplifying the pulsed power systems. Additionally, the very low cost of PLIA is a major advantage of this concept [1].

The PLIA consists of a helix wound over an evacuated beam tube, an outer dielectric layer and an outer conductor. A ramped voltage waveform is applied to a helical pulse line creating a traveling wave which produces an accelerating electric field to the ions over the length of the helix. The basic parameters of the Lanzhou Test PLIA (LTP) are listed in Table 1. The input voltage waveform and the corresponding accelerating electric field waveform are shown in Fig. 1. The accelerating electric field is $E=\frac{2V_0}{l_t}=\frac{2V_0}{v_t\tau_t}$, where V_0 is the input voltage of PLIA, l_t is the ramp region where the voltage goes from V_0 to $-V_0$, v_t is the wave velocity and τ_t is the ramp-up time [2].

Table 1. The basic parameters of LTP.

parameter	value
vacuum insulator radius/mm	26
helix radius/mm	30.6
ground return radius/mm	44
helix pitch/(turns/m)	783
effective helix length/mm	700
relative permittivity(oil)	2.3
capacitance/(pF/m)	351
inductance/(μH/m)	1160.8
impedance/Ω	1820
wave velocity/(m/s)	1.57×10^6

Received 7 September 2011
* Supported by National Natural Science Foundation of China (10921504, 11105197)
1) E-mail: shenkang198@impcas.ac.cn
2) E-mail: zzm@impcas.ac.cn

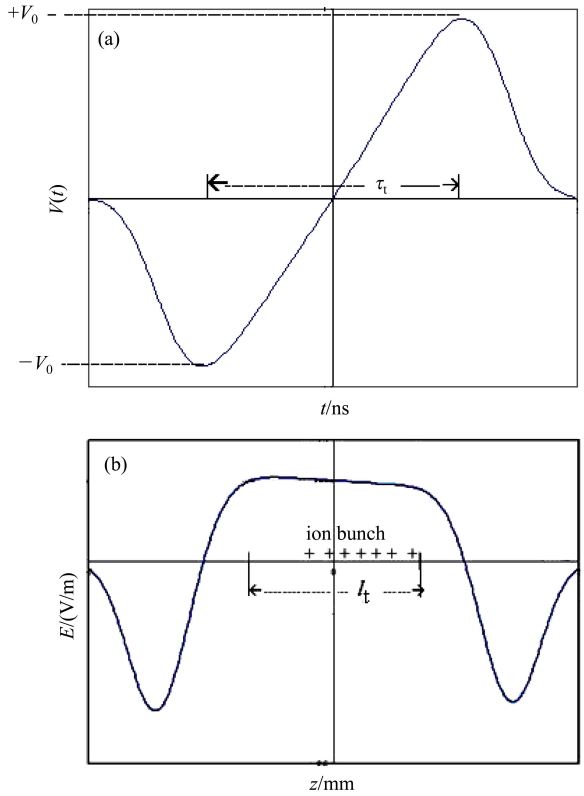

Fig. 1. (a) The input voltage waveform; (b) The accelerating electric field waveform.

2 The electric field simulation of PLIA

The proof-of-principle experiment of PLIA has been done by LTP, and the measured traveling wave velocity agrees well with the calculated result [3]. In order to make a reference for the subsequent ion acceleration experiment, it is necessary to simulate and measure the electric field of the PLIA.

The simulations were performed by CST which is a general-purpose electromagnetic simulator based on the finite integration technique. If the actual parameters are used in the simulation, the size of time-step and mesh requires an unreasonably long computational time. Therefore a scaling relation is proposed to make the simulation faster [4]. The wire-spacing used in the simulation is 5 times larger than that used in the real experiment. The velocity of the traveling electromagnetic waveform is also increased with larger wire spacing. Therefore, the theoretical calculation of the wave velocity should be 7.85×10^6 m/s, and the corresponding electric field is 7.6 kV/m.

The theoretical input voltage, which is shown in Fig. 1, is ideal, the voltage from $-V_0$ to V_0 increases linearly, so the corresponding accelerating electric field will have a platform. However, the real input voltage does not increase linearly; it is a near-sinusoidal voltage signal. So the platform of the accelerating electric field is not obvious. In order to compare the simulation with the actual situation, the real voltage waveform is used as the excitation signal in the simulation. Fig. 2 is the waveform of the input voltage and accelerating electric field in the simulation. The peak value of the accelerating electric field is about 11 kV/m, which is a little larger than the calculated result. The reason for this may be that the real input voltage waveform is near-sinusoidal, rather than a linear upward, so the linear ramp-up time is shorter than the actual 85 ns. Additionally, the amplitude of the electric field will be larger than the calculated value.

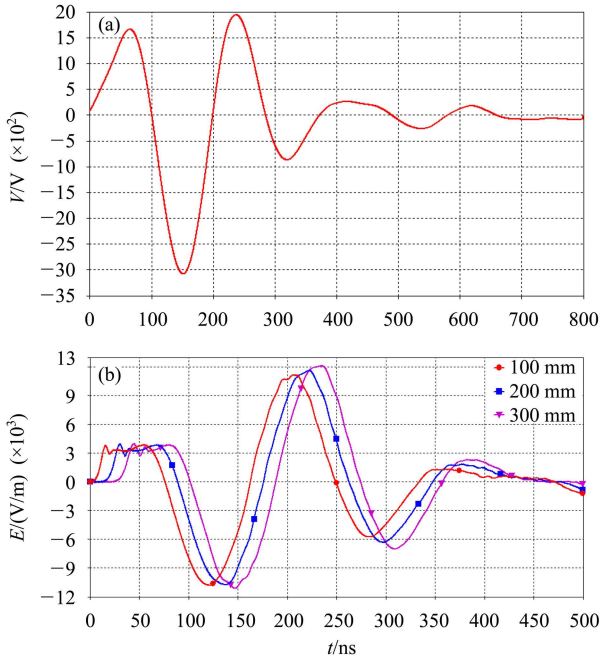

Fig. 2. (color online) (a)The waveform of input voltage; (b)The accelerating electric field in the simulation.

The amplitude of E on axis is similar to that on the insulator surface for a frequency satisfying $ka \ll 1$, where k is the wave number and a is the helix radius. Fig. 3(a) shows the amplitudes of E on axis and on the insulator surface for f=6 MHz ($ka \ll 1$). However, when the frequency is higher ($ka \gg 1$), the amplitude of E on insulator surface is much greater than that on axis [4]. Fig. 3(b) is the amplitudes of E on the axis and on the insulator surface for f=100 MHz

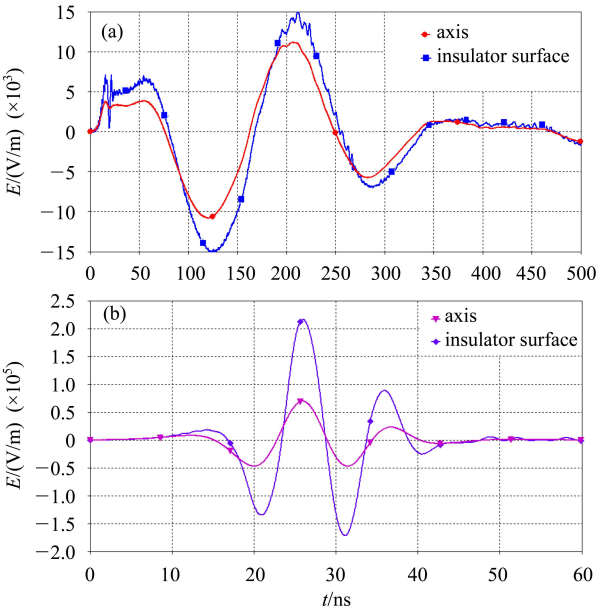

Fig. 3. (a) The amplitudes of E on the axis and on the insulator surface for f=6 MHz; (b) f= 100 MHz.

($ka \gg 1$). It shows that the high frequency modes will generate a high electric field on the insulator surface, which may lead to the insulator flashover. So the high frequency modes should be removed from the input voltage signal in order to avoid the insulator flashover.

3 Electric field measurement

3.1 Types of electric field sensors

The traditional sensor for an electric field is the metal spherical dipole. In this method, the electric field signal is obtained directly by the dipole antenna, and is then transported through coaxial cables to the oscilloscope for display. This method is simple, but it is difficult to precisely measure such an intensive transient electric field without disturbing the distribution of the electric field, because the high E-field may have a strong effect on the coaxial cable which connects the sensor to the signal meter. The metal material of the sensor also greatly distorts the field.

In another system, optical fibers are used to transport the signal, which should greatly improve the quality and veracity of signals. The basic structure is as follows. In the sensor-head there is a dipole antenna which is connected with the optical fiber system through electro-optic modulation. In the receiving end a photoelectric conversion is conducted and the time-domain waveform could be observed in the oscilloscope. It needs to provide a battery for the electro-optic modulation in the sensor-heads, so it is named the active electro-optic sensor. This method also has some disadvantages [5]. Firstly, this measurement system is so active that it will be seriously affected by the electric field. Secondly, this type of sensor will disturb the distribution of the electric field according to its metal material. Thirdly, the size of the sensor is quite big so it cannot be used in precise measurements. Also, the capacity of the battery inside limits its operation.

An integrated electro-optic field sensor using crystal substrates to measure a high power impulse electric field has been developed in recent years [6]. Compared with conventional sensors, the integrated sensor has the advantage of compact-size, broad band response and a large measurement range. Additionally, the influence on the electromagnetic field is reduced because most of the sensor materials are nonmetallic. This sensor is passive, so it will have no effect on the measured electric field, and the operating time of the sensor is unlimited.

3.2 Electric field measurement sensor for LTP

Based on lots of investigations and comparisons, an integrated electro-optic field sensor is adopted to measure the electric field. The optical electric integrated electric field sensor, which was developed by the Department of Electrical Engineering, Tsinghua University, has a very small size (7 cm×1 cm×1 cm), an intensive electric field measurement range (-10^6–10^6 V/m), a wide pass band (1 GHz), and it can measure the electric field in one direction only [6]. Therefore, it is suitable to measure the electric field of the PLIA.

The structure of the sensor is illustrated in Fig. 4. There is a path difference of one-quarter of the wavelength of light between these two arms in order to form an optical bias of $\pi/2$, which is desirable for the output of the sensor to be linear with the input electric field. The refracting index of some electro-optic crystals will change when an electric field is put on it, which will cause the phase shift of the light wave. According to the fundamental principle of the Mach-Zehnder modulator, the modulator output of optical power can be expressed as $P_o = \frac{P_i}{2}(1-\sin\varphi)$, so the value of electric field can be acquired by measuring the output laser power [7].

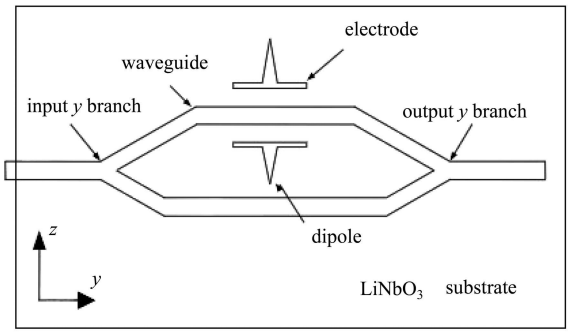

Fig. 4. The structure of the sensor.

3.3 The electric field measurement system for LTP

The configuration of the measurement system is illustrated in Fig. 5. It has four parts: a laser source, an optical electric integrated electric field sensor, an optical receiver and a signal processing system. A 50 m-long polarization maintaining fiber (PMF) connects the sensor to the optical laser source, and a 50 m-long single mode fiber (SMF) connects the sensor to the optical receiver. The input laser signal is modulated in the optical electric integrated electric field sensor by the measured electric field. The amplitude of the output optical signal is measured by the optical receiver and converted to an electrical signal which is suitable for analysis with an oscilloscope or another signal processor [5]. In order to avoid the environmental electromagnetic interference, the laser source, optical receiver and signal processing system were placed in an electromagnetic shielding room.

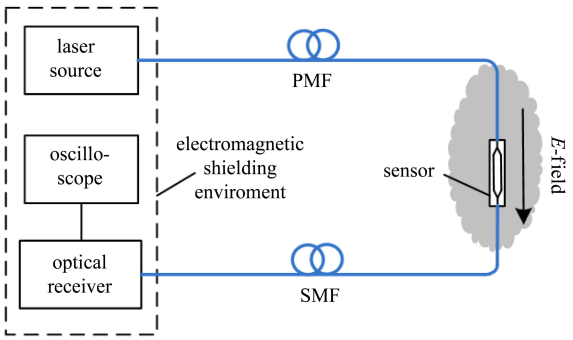

Fig. 5. The configuration of the measurement system.

3.4 The electric field measurement results

The axis electric field at different locations along the helix is shown in Fig. 6. The electric field is almost the same at different locations, and the waveforms are consistent with the simulation results. This shows that the electric field is almost loss-free during the propagation. But the amplitude is smaller than the calculated value of 37 kV/m. The possible reason for this is described as follows. The helix inductance decreased at both ends because the mutual coupling from the neighboring turns was lower at both ends of the helix. To approximate the mutual inductance from later turns, a string of resisters in a spiral with a pitch similar to the helix was used on the oil dielectric helix [8]. The simulation results show that the electric field amplitude decreased to 20 kV/m when the resister was not wrapped. Due to the space limitation at both ends of the helix and the volume limitation of the resister, the actual pitch of the resister column is much less than that of the helix. So the electric field will be decreased in this situation. A new helix configuration in which the pitch of resister column will be increased to be similar to the helix is being constructed to resolve this problem.

Figure. 7 is the comparison of electric field on the axis and on the insulator surface for a low frequency. The amplitude of the electric field on the axis is similar to that on the insulator surface, which matches the simulation result.

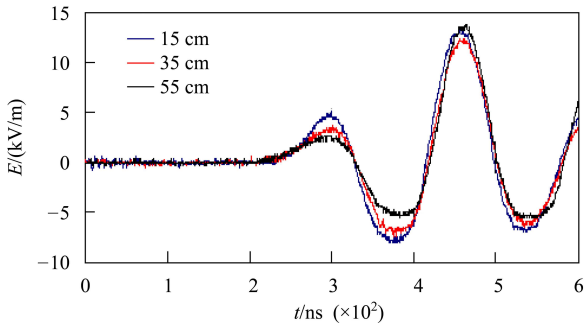

Fig. 6. (color online) The electric field on the axis at different locations along the helix.

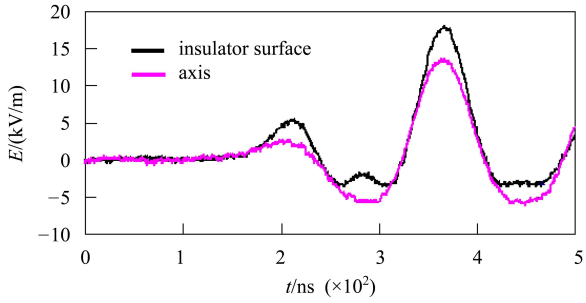

Fig. 7. (color online) The comparison of the electric field on the axis and on the insulator surface for low frequency.

4 Conclusion

The simulation results show that high frequency modes which may lead to the insulator flashover should be removed from the input voltage signal to avoid the insulator flashover. The electric field measurement result, which is completed by the optical electric integrated electric field measurement system provides an important reference for the subsequent ion acceleration experiment. The real altitude of the axial electric field is smaller than that of the calculation, probably due to the actual pitch of the resister column which is much less than that of the helix. This will be tested by increasing the pitch of the resister column to be similar to the helix in the new helix configuration which is being constructed to resolve this problem.

References

1 Briggs R J. Physical Review Special Topics-Accelerators and Beams, 2006, **9**(6): 060401

2 Colemana J E, Friedmanb A et al. Nuclear Instruments and Methods in Physics Research Section A, 2007, **577**: 197–202

3 SHEN Xiao-Kang, CAO Shu-Chun, ZHANG Zi-Min et al. Chinese Physics C (HEP & NP), 2012, **36**(3): 241–246

4 LING C Y, YU S S, Henestroza E. Nuclear Instruments and Methods in Physics Research Section A, 2009, **606**: 102–106

5 NIU Ben, ZENG Rong, GENG Yi-Nan, HE Jin-Liang et al. An Electro-Optic Integrated Sensor for Lightning Impulse Electric Field Measurements. 19th International Zurich Symposium on Electromagnetic Compatibility. http:// ieeexplore.ieee.org/xpl/freeabs_all.jsp?arnumber=4559874

6 ZENG Rong, CHEN Wei-Yuan, HE Jin-Liang et al. High Voltage Engineering, 2006, **32**(7): 1–5

7 ZENG Rong, CHEN Wei-Yuan, HE Jin-Liang. The Development of Integrated Electro-optic Sensor for Intensive Electric Field Measurement. IEEE International Symposium on Electromagnetic Compatibility. http:// ieeexplore.ieee.org/xpl/freeabs_all.jsp?arnumber=4305629

8 Waldron W, Reginato L, Briggs R J. High Voltage Operation of Helical Pulseline Structures for Ion Acceleration. In: Horak C ed. Proceedings of the 2005 Particle Accelerator Conference. Knoxville. 2005. 440. http://accelconf.web.cern.ch/AccelConf/p05/PAPERS/ROAB005.PDF